Infectious Disease Modelling 10 (2025) 129–138

Contents lists available at ScienceDirect

Infectious Disease Modelling

journal homepage: www.keaipublishing.com/idm

Impact of vaccination on Omicron's escape variants: Insights from fine-scale modelling of waning immunity in Hong Kong

Yuling Zou [a], Wing-Cheong Lo [b], Wai-Kit Ming [c], Hsiang-Yu Yuan [a, d, *]

[a] *Department of Biomedical Sciences, Jockey Club College of Veterinary Medicine and Life Sciences, City University of Hong Kong, Hong Kong, China*
[b] *Department of Mathematics, City University of Hong Kong, Hong Kong, China*
[c] *Department of Infectious Diseases and Public Health, City University of Hong Kong, Hong Kong, China*
[d] *Centre for Applied One Health Research and Policy Advice, Jockey Club College of Veterinary Medicine and Life Sciences, City University of Hong Kong, Hong Kong, China*

A R T I C L E I N F O

Article history:
Received 14 May 2024
Received in revised form 26 August 2024
Accepted 14 September 2024
Available online 16 September 2024
Handling Editor: Raluca Eftimie

Keywords:
COVID-19
Epidemic model
Waning immunity
Immune-escape
Discrete-time simulation

A B S T R A C T

COVID-19 vaccine-induced protection declines over time. This waning of immunity has been described in modelling as a lower level of protection. This study incorporated fine-scale vaccine waning into modelling to predict the next surge of the Omicron variant of the SARS-CoV-2 virus. In Hong Kong, the Omicron subvariant BA.2 caused a significant epidemic wave between February and April 2022, which triggered high vaccination rates. About half a year later, a second outbreak, dominated by a combination of BA.2, BA.4 and BA.5 subvariants, began to spread. We developed mathematical equations to formulate continuous changes in vaccine boosting and waning based on empirical serological data. These equations were incorporated into a multi-strain discrete-time Susceptible-Exposed-Infectious-Removed model. The daily number of reported cases during the first Omicron outbreak, with daily vaccination rates, the population mobility index and daily average temperature, were used to train the model. The model successfully predicted the size and timing of the second surge and the variant replacement by BA.4/5. It estimated 655,893 cumulative reported cases from June 1, 2022 to 31 October 2022, which was only 2.69% fewer than the observed cumulative number of 674,008. The model projected that increased vaccine protection (by larger vaccine coverage or no vaccine waning) would reduce the size of the second surge of BA.2 infections substantially but would allow more subsequent BA.4/5 infections. Increased vaccine coverage or greater vaccine protection can reduce the infection rate during certain periods when the immune-escape variants co-circulate; however, new immune-escape variants spread more by out-competing the previous strain.

* Corresponding author. Department of Biomedical Sciences, Jockey Club College of Veterinary Medicine and Life Sciences, City University of Hong Kong, Hong Kong, China.

E-mail address: sean.yuan@cityu.edu.hk (H.-Y. Yuan).

Peer review under responsibility of KeAi Communications Co., Ltd.

https://doi.org/10.1016/j.idm.2024.09.006

1. Introduction

Even though the public health emergency of the COVID-19 pandemic was declared over in 2023 along with mass vaccination programmes (World Health Organization, 2023), certain factors continue to influence the dynamics of the disease, such as waning immunity and the emergence of new immune-escape variants of the virus that caused COVID-19, severe acute respiratory syndrome coronavirus 2 (Levin et al., 2021; Najar et al., 2023; Peng et al., 2022; Thompson et al., 2021). While modelling approaches are commonly used to make predictions regarding vaccination (Bubar et al., 2021; Liu et al., 2022; Mahmud et al., 2022), most of these assume that vaccine protection declines at a constant rate to certain fixed levels after the immunity has waned. Hence, vaccine protection over the days that have passed since the last injection is not traced. Incorporation into modelling of fine-scale immune responses, such as daily changes in vaccine protection and immune-escape properties, is expected to improve a model's predictive ability in preparation for the re-emergence of the outbreak (Smith et al., 2021).

Hong Kong faced a significant health burden due to Omicron infections. BA.2 first entered the community in December 2021 and its spread resulted in an epidemic peak of the fifth wave around mid-March 2022 (about 60,000 cases per day) (Yuan et al., 2022). After the outbreak had been contained, the daily number of cases became consistently low (below 1000) between April and June. Although many people developed immunity through natural infection and vaccination, there was a second surge in June 2022, caused by the co-circulation of BA.2 with BA.4 and BA.5 (denoted as BA.4/5). By the end of October 2022, circulation of BA.2 had declined and BA.4/5 mutant viruses predominated (The Government of Hong Kong Special Administrative Region, 2022a). The BA.4/5 variants have a greater potential to escape vaccine protection and stronger transmissibility than BA.2 and thus are more likely to cause vaccine breakthrough infections (Chen et al., 2023).

Before the significant growth of the fifth wave, many people in Hong Kong had not completed the full immunisation programme (i.e. the first two doses of vaccine). In response of the outbreak, many people got vaccinated (Yuan et al., 2022). Two brands of vaccine (BNT162b2 and SINOVAC) were available. The different vaccine brands and doses varied in their rates of waning immunity, but in general, the two-dose vaccine protection began to decline a few months after injection. Three doses of BNT162b2 provided adequate protection, but three doses of SINOVAC produced only limited protection (Lau et al., 2024).

The study aimed to incorporate fine-scale waning immunity into epidemic modelling to predict the second surge of the outbreak and to understand the impact of vaccine waning on the replacement of BA.2 by the new immune-escape variants.

2. Data and methods

2.1. Data sources

Our study focused on the fifth epidemic wave of COVID-19 in Hong Kong, which began in December 2021. We collated epidemiological data from publicly available data sources; the numbers of COVID-19 BA.2 cases that were reported daily in Hong Kong from December 25, 2021 to October 30, 2022 (the study period) were collected from the local COVID-19 thematic website (The Government of Hong Kong Special Administrative Region, 2022b). After August 1, 2022, daily figures for the reported mutations BA.4/5 were estimated by multiplying the daily proportions of different cases, reported in press release from the Department of Health (2022) by the numbers of total cases, also reported daily. The daily numbers of vaccinations (the first/second/third doses) were collected from 2022, a portal through which users can access open data from the Hong Kong Government. The data that were used to estimate the vaccine protection function with waning immunity were taken from previous studies (Chen et al., 2023; Lau et al., 2024).

Daily mean temperatures during the study period were collected from the Kong, 2022. The daily average mobility index for Hong Kong between December 25, 2021 and October 15, 2022 was collected from Our World in, 2022. The mobility data from October 16, 2022 to 31 October 2022 were estimated using the average mobility index from 15 August to October 15, 2022. Other data, such as the values of some parameters from previous studies, are listed in Supplementary Table S3.

2.2. Study flow

First, we developed mathematical formulae to represent the boosting and waning of vaccine-induced protection. The pattern of waning immunity was obtained after fitting the formulae to the vaccine protection information, which was derived from serological data. Next, we developed a two-strain Susceptible-Exposed-Infectious-Removed (SEIR) model embedding the boosting and waning of vaccine protection using discrete-time simulation. The model was trained using the daily number of cases that occurred during the first outbreak driven by Omicron BA.2. Then the trained model was used to predict the second outbreak, which was driven by the strains BA.2 and BA.4/5. The model was used to simulate the dynamics of the outbreak with and without waning immunity, and the results were compared (see Fig. 1A for the study flow).

2.2.1. Formulation of vaccine waning immunity

A generalised growth and decay function combined with exponential components (Menegale et al., 2023) was developed from empirical serological data to represent the changing protection from the j th dose over time (Chen et al., 2023; Khoury et al., 2021; Lau et al., 2024). The protections from the second and third doses were formulated as follows:

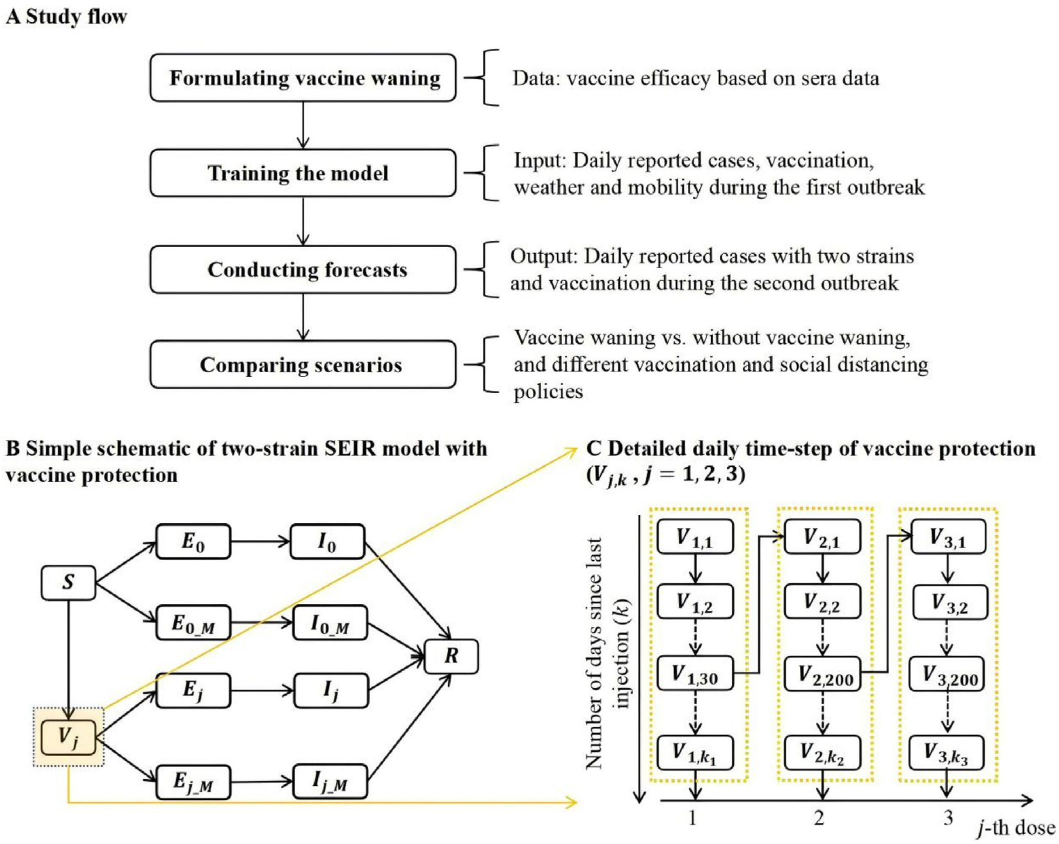

Fig. 1. Model schematic and study flow. (A) The whole study flow. (B) A simple schematic of the SEIR model with vaccine waning. Individuals were classified into the following groups: S (Susceptible, without any vaccination and had never been infected), V (Vaccinated), E (Exposed but not yet infected), I (Infectious), and R (Recovered, including hospital confirmed, recovered and removed). (C) Detailed daily time-step of vaccine protection in vaccinated individuals V in Fig. 1B. The subscripts j and k represent the status of individuals who have received the jth dose since k days ago.

$$P_{j,k_j} = c_j \bullet Boosting(k_j) \bullet Waning(k_j) (j = 1, 2, 3) \tag{1}$$

where P_{j,k_j} was vaccine protection; $j = 1, 2, 3$ was the number of doses; and k_j was the number of days since the injection of the jth dose. The function $k_1 \in [1, 30]$ represented the first dose and $k_j \in [1, 200]$ when $j = 2, 3,$ the second and third doses. We split the change of protection into two parts: immune boosting and waning. $Boosting = 1 - exp(-a(k_j - 1))$, which represented the increase of protection. The factor a was formulated such that when $a = \frac{ln(x)}{m-1}$, the boosting protection reached $(1 - x^{-1}) \times 100\%$ on the m th day. For example, if we assumed that $x = 50$ and $m = 7$, the protection would reach 98% after seven days if immunity did not wane (Fig. 2A). $Waning = exp(-b(k_j - 1))$, which represented the decrease of protection. The factor b was formulated such that when $b = \frac{ln(x)}{m-1}$, the protection waned to $(x^{-1}) \times 100\%$ on the m th day. If individuals received three doses of BNT162b2, we assumed that the waning protection remained 1/3 on the 90th day: $b = \ln 3/89$. If these individuals took other vaccination regimens, we assumed that the waning protection remained 1/4 on the 90th day: $b = \ln 4/89$, which means that the immunity of these vaccination regimens waned at a faster rate (Fig. 2B). The factors a and b controlled the levels of the boosting and waning functions. The factor c_j was a scaling factor that set the maximum level of vaccine protection from the j th dose.

The vaccine protection reached a maximum on the seventh day after injection and decreased by about 70% after 100 days (Fig. 2CD). The maximum vaccine protection if there was no waning mechanism, represented by c_j, was estimated by the least square method using data that are shown in Supplementary Tables S1 and S2. The average level of protection from different vaccine regimens was used to represent the vaccine protection in the population in our model (Supplementary Table S3, The proportions of different vaccination schemes).

2.2.2. Infectious disease modelling

The time-varying transmission rate β was determined by several factors, such as vaccine protection, temperature and population mobility:

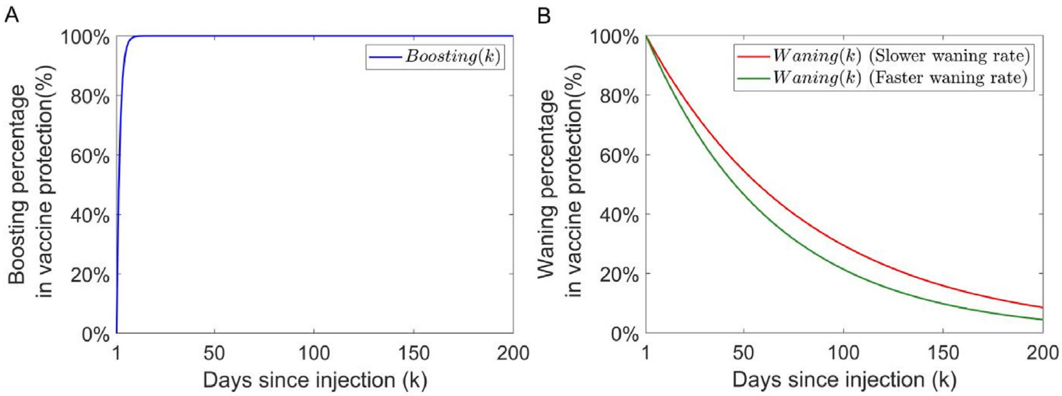

Fig. 2. The waning and boosting tendencies of vaccine protection. (A) Boosting tendency of vaccine protection after injection. (B) Waning tendency of vaccine protection after injection for two different conditions. The red curve represents individuals who had received three doses of BNT162b2, for whom the waning protection remained 1/3 on the 90th day: $b = \ln 3/89$. The green curve represents individuals taking other three vaccine regimens (two doses of BNT162b2, two doses of SINOVAC and three doses of SINOVAC) with a faster waning rate, for whom the waning protection remained 1/4 on the 90th day: $b = \ln 4/89$.

$$\beta^t_{j,k_j} = C_0 \bullet \left(1 - P_{j,k_j}\right) \bullet \rho_0 \bullet W_t(T_t) \bullet M_t \tag{2}$$

in which subscripts j and k denoted that individuals had received the jth dose k days previously; and C_0 was the average number of contacts per person per day (Liang et al., 2022); P_{j,k_j} was the vaccine protection (see eq. (1)); ρ_0 was the estimated probability of successful infection after each contact with BA.2; W_t represented the non-linear effect of daily temperature T_t on the transmission rate (Supplementary Fig. S1AC). M_t was the daily average mobility rate (Supplementary Fig. S1B) (Our World in, 2022);

A two-strain model with waning immunity of vaccines was developed based on an SEIR framework (Fig. 1B) (Dick et al., 2021; He et al., 2020). The use of discrete-time simulation enabled the model to track the number of doses and days since the last infection among vaccinated individuals (Fig. 1C). We assumed that the numbers of people who received their first vaccine doses were set according to the actual data before March 26, 2022 (the end date of the fifth epidemic wave: the number of daily new cases was lower than 10,000) and as 1% of the number of the daily S group after that period. Based on the average dose interval (i.e. 30 days after the injection of the first dose), the model calculated the numbers of people who received their second or third doses each day and had not been infected. After March 5, 2022, the average interval between the second and third doses was shortened from 200 to 90 days for the general population (who would receive their second doses after March 5, 2022) (The Government of Hong Kong Special, 2022) while that interval for some special groups (e.g. infants, adolescents aged between 12 and 17 years who received two doses of BNT162b2 vaccine, and pregnant women) remained unchanged at 200 days. We assumed that 10% of the population belonged to the special groups (Supplementary Fig. S2, Mathematical expression of discrete-time vaccinated SEIR model).

The model assumed that the probability of being infected with BA.4/5 (ρ_M; see Supplementary: Cross immunity model) was about 1.5 times that for BA.2 (ρ_0; see eq. (3)) (Esterman, 2022). Meanwhile, the mutations BA.4/5 were more likely to escape the protection provided by vaccines. Thus, we assumed that one or two doses of vaccine did not induce protection against BA.4/5 (Chen et al., 2023; Pérez-Then et al., 2022), so it was assumed that the protection of one or two doses of vaccine against BA.4/5 disappeared. Based on the above literature data (Chen et al., 2023), a new formulation of waning immunity from three doses of SINOVAC against BA.4/5 was constructed. It was known that individuals were infected with only one of these three subvariants (BA2 or BA.4/5) and those who recovered developed very strong protection against both these mutations, at least during the study period (i.e. between January 2022 and October 2022) (Fig. 1B).

2.2.3. Model training and forecast

For training, we fitted the model to the daily number of reported cases during the first Omicron outbreak, between December 25, 2021 and April 22, 2022 (the training period) and took into account other factors (i.e. weather and mobility). Next, the parameterised model was used to predict the daily numbers of cases with BA.2 and with BA.4/5, as well as the number of individuals who received each vaccine dose between April 23, 2022 and 31 October 2022 (the prediction period). The model assumed that 38% of infectious cases were detected and reported, in line with previous studies (Yuan et al., 2022; Lau et al., 2024). In addition, a null model that did not include waning immunity (i.e. with constant vaccine protection) was developed for comparison, to validate the effect of the gradual change in immunity. The null model was trained during the same training period.

Finally, we projected outbreak dynamics under three scenarios with different combinations of interventions.

(1) the social distance policy was strengthened, so that the mobility index was decreased by 10% from 1 September to 30 September compared with the original forecast data;
(2) vaccine coverage was increased with a booster dose to ensure that 100% of those people who had never been infected completed three doses. This intervention aimed to explore whether a larger scale of vaccine coverage combined with the recovered group could control the spread of new variants; and
(3) both of the above measures were implemented simultaneously.

3. Results

3.1. Vaccine protection taking account of waning immunity

The empirical patterns of vaccine waning immunity were reproduced using mathematical formulae. The level of vaccine protection rose and reduced differently across a variety of injection regimens. Two doses of either of the two brands induced relatively low protection against BA.2 (Fig. 3A). The booster dose increased protection but the effect waned after a few months. For example, the maximum level of vaccine protection from three doses of BNT162b2 reached 45.33%, and this declined to 14.68% after 100 days (Fig. 3B). Additionally, this vaccine was less effective against BA.4/5 compared with BA.2. The highest average protection from the three-dose vaccine reached 42.11% against BA.2 but this protection level was reduced to 10.72% against BA.4/5 (Fig. 3CD).

3.2. Predictions of vaccination rates and the second outbreak

Before training the model, we validated the predictions of vaccination rates. The predicted numbers of total daily injections of the second and third doses of vaccine successfully captured the actual daily numbers of these doses during the first outbreak at the required dosage intervals (Fig. 4AB). The numbers of second doses were markedly higher than those of third doses during the study period (Fig. 4C). To improve the prediction of the daily numbers of third doses, the probability that

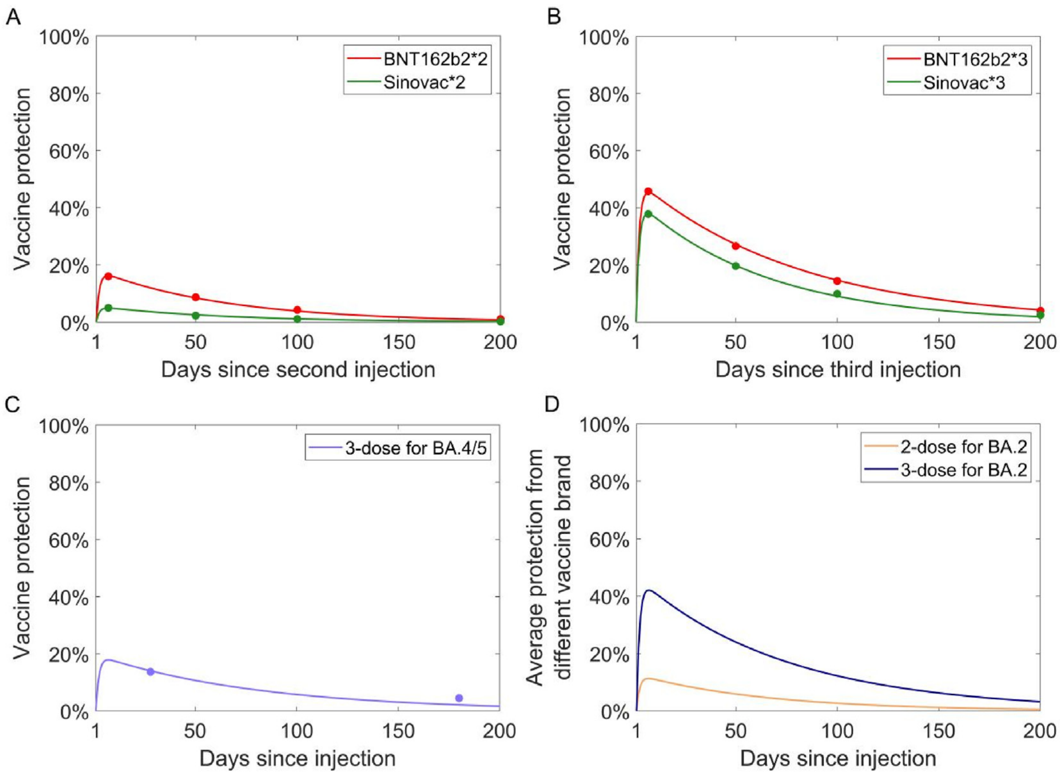

Fig. 3. Changes in vaccine protection. (A) The modelled vaccine protection curves of two doses over time. The red curve represents the estimated protection of two doses of BNT162b2 and the green curve represents the estimated protection of two doses of SINOVAC. $b = \ln 4/89$ for both curves. (B) The modelled vaccine protection curves for three doses. The curves represent the model's estimated protection after the third dose using different vaccination brands. $b = \ln 4/89$ for the green curve and $b = \ln 3/89$ for the red curve. (C) The protection against mutations BA.4/5 from three doses of vaccine. All circular data points presented in Fig. 3ABC are observed vaccine protection data from references (Chen et al., 2023; Lau et al., 2024). (D) Weighted average vaccine protection from different vaccine brands against variant BA.2. The orange curve is the mean of the two curves in A. The solid blue curve is the mean of the four curves in B.

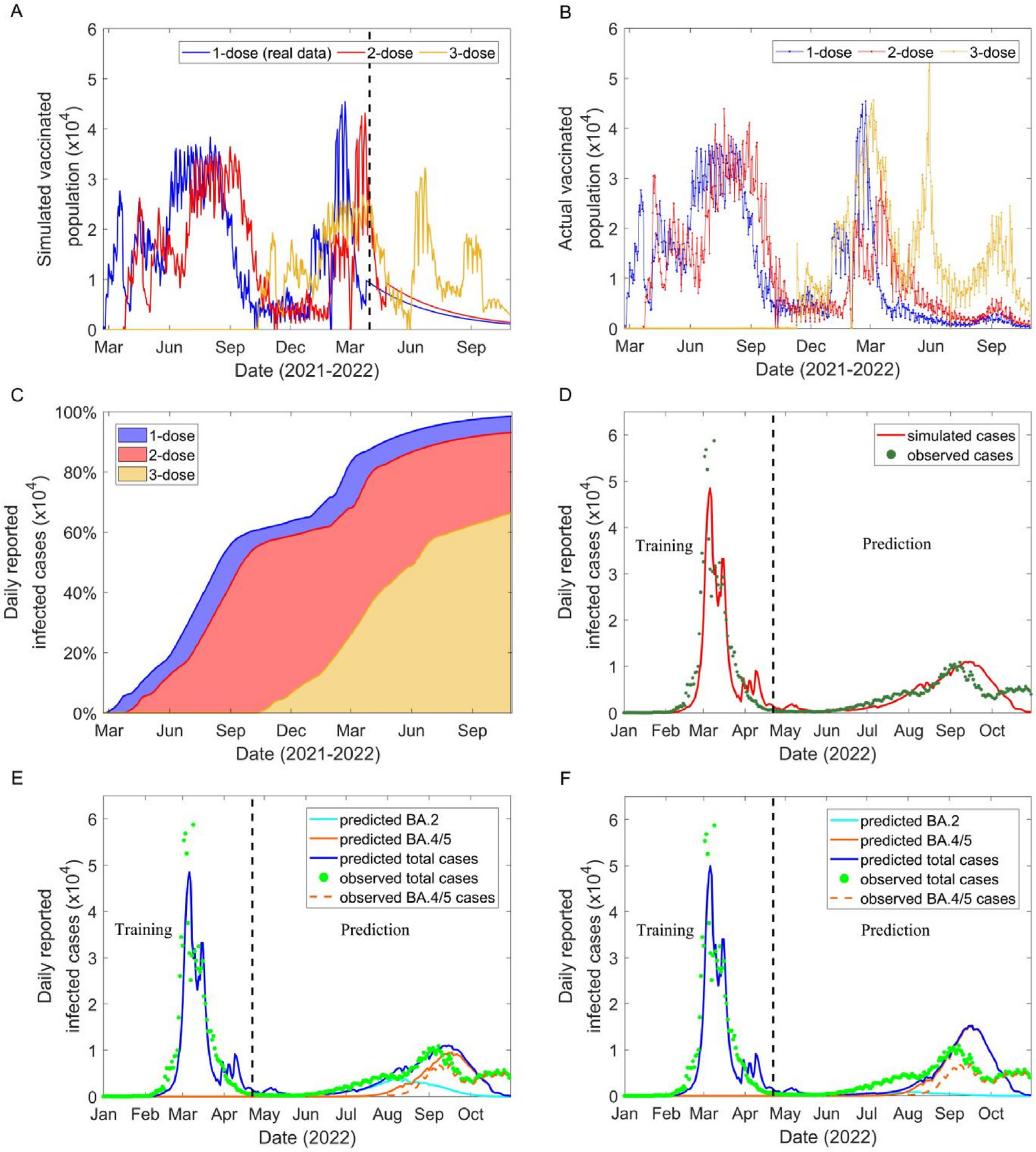

Fig. 4. Training of the model and its predictions of the dynamics of vaccination and transmission. (A) Predicted daily numbers of vaccinations. The daily number of first-dose injections before the vertical dashed line was used to simulate the number of vaccinations of other doses or during the other period (i.e. after the dashed line). (B) Observed daily numbers of vaccinations. (C) Daily vaccine coverage. (D) Model-simulated transmission dynamics during the training (i.e. before the vertical dashed line) and prediction (i.e. after the vertical dashed line) periods. The solid red curve represents the simulated daily numbers of reported infectious cases (under the detection rate of 38%) when waning immunity was taken into account. The green points represent the observed numbers of daily reported cases. (E) The model-simulated transmission dynamics with waning immunity (detailed subgroups in D). (F) The model-simulated transmission dynamics without waning immunity.

susceptible individuals with full immunisation would get booster doses after the required time interval was set to 70%. It is worth noting that, during our model simulation, to separate the protective effect of vaccination from rates of natural infection, only people who had been vaccinated without being previously infected were tracked. The protection of vaccinated individuals who were later infected was determined by natural infection.

After incorporating the varying numbers of doses, the model successfully predicted the trend of the evolution of COVID-19's second surge that followed the fifth epidemic wave, including its size and arrival date (Fig. 4D). In the model outcome, this surge resulted in cumulative reported cases of 655,893 people (8.77% of the population) between June 1, 2022 and 31 October 2022. This figure was only 2.69% less than the observed cumulative number of 674,008. Furthermore, the epidemic peak was predicted to occur on 15 September with 11,030 daily reported cases; this prediction was comparable with the observed peak on 8 September with 10,910 daily reported cases (Fig. 4D).

The second surge involved the co-circulation of variants BA.2 and BA.4/5, with BA.4/5 being the dominant strain (Fig. 5A). There were two hidden sub-peaks, each associated with a different variant: BA.2 reached a relatively lower peak in early August (9 August, 4059 cases), while BA.4/5 reached a higher peak in mid-September (18 September, 9455 cases). These separate peaks can be explained by many people being infected during the initial fifth wave, a large number of whom recovered. This increased community protection and led the second surge to be smaller than the first (Fig. 4D). Additionally, vaccination was more effective at suppressing BA.2 but less protective against BA.4/5 (Fig. 5A).

3.3. Impacts of vaccine waning on the spread of immune-escape

To verify the impact of waning immunity, a null model that did not take it into account was developed for comparison. Under this alternative hypothesis, the average levels of protection of the second and third doses of vaccines were maintained at the maximum values. It was found that the null model did not capture the actual transmission dynamics well. Without waning immunity, the level of the early second surge caused by BA.2 was lower. However, a larger outbreak was actually observed occurred in the model after BA.4/5 emerged with a delay (Fig. 4EF). When waning immunity was considered, the protection against BA.4/5 among vaccinated individuals who had not been infected was initially lower than that shown in the null model before the second surge of BA.2, but the population immunity rose more quickly due to the second surge (Supplementary Fig. S4).

3.4. Impacts of control measures on the spread of immune-escape

We projected the second surge under three different social distancing and vaccination scenarios and compared the outcomes with those that were found under the previous settings (Table 1). In the first scenario, when population mobility was reduced by 10% (compared with the observed data) between September 1, 2022 and September 30, 2022, the number of cases was reduced by 10.03% during the period (Table 1 and Fig. 5B). The number of cumulative cases of BA.2 was reduced by 2.23% and the number for BA.4/5 was reduced by 13.38%. In the second scenario, the probability that all susceptible individuals with full immunisation would get booster doses after the required time interval was increased from 70% to 100%

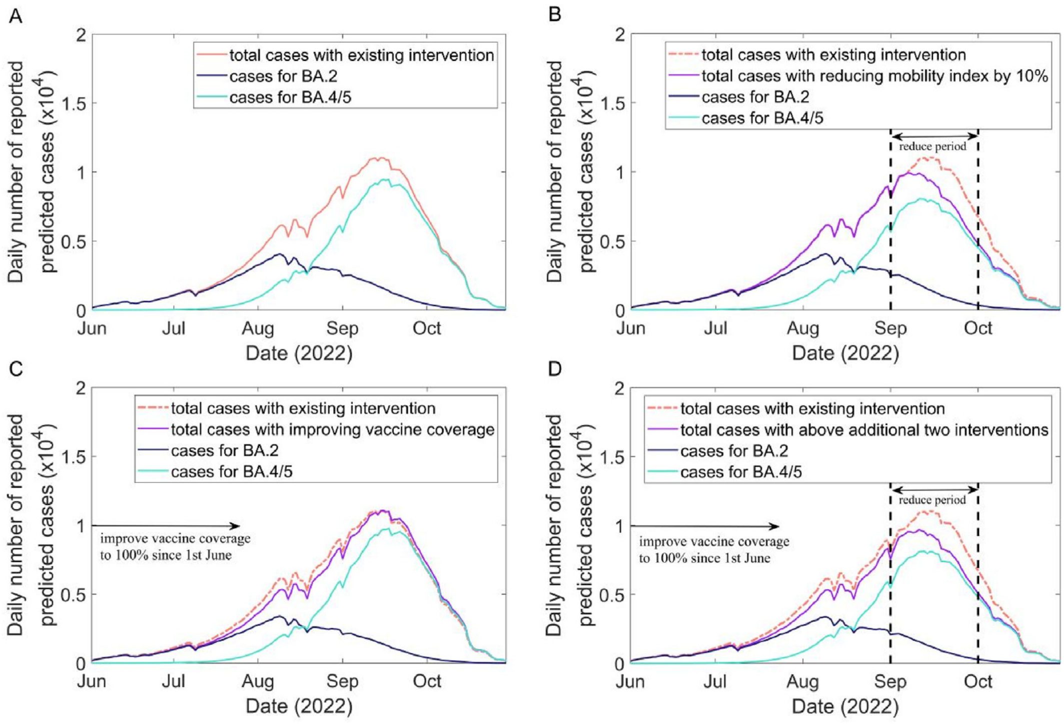

Fig. 5. Model projections with different levels of intervention for variants BA.2 and BA.4/5. (A) The numbers of predicted infectious cases with certain interventions and under actual interventions. The figure is an extension of Fig. 4D. (B) Results of modelled implementation of stricter social distancing policy. The two vertical dashed lines represent the period (1 September-30 September) when the mobility index was reduced by 10%. The pink line represents the predicted case with intervention, purple dashed line represents the original predicted cases without any intervention. (C) Vaccine coverage of booster doses is improved to 100%. The model assumed that the population would be fully vaccinated through booster doses after 1 June. (D) Results of modelling of implementation of both more stringent social distancing and total booster dose coverage policies. Vertical dashed lines indicate the same period as (B) when the social distancing policy is tightened.

Table 1
Cumulative cases of COVID-19 during the second surge under different control measures. The predicted numbers of cases between June 1, 2022 and 31 October 2022 were calculated. Percentage changes in the numbers of cases compared with the existing interventions are shown.

	#Total cases	#Cases (BA.2)	#Cases (BA.4/5)
Existing interventions	655893	229756	426138
10% reduced mobility index (between 1 Sep. and 30 Sep.)	593745 (−9.48%)	224642 (−2.23%)	369103 (−13.38%)
100% vaccine coverage (after June 1, 2022)	631152 (−3.77%)	197526 (−14.03%)	433627 (+1.76%)
Combination of the two interventions above	565953 (−13.71%)	193039 (−15.98%)	372914 (−12.49%)

after 1 June. A 3.77% reduction in the number of cumulative cases during this period was observed (Table 1 and Fig. 5C). Under this scenario of complete vaccine coverage, the number of cumulative cases due to BA.2 was reduced significantly (−14.03%), but the cumulative number due to BA.4/5 was slightly increased (+1.76%). If both the social distance policy and achievement of higher vaccination coverage were implemented, the number of cases due to BA.2 was reduced by 15.98% and those due to BA.4/5 were reduced by 12.49%, resulting in a 13.71% reduction in the total number of cases during the second surge (Table 1 and Fig. 5D).

3.5. Sensitivity analysis (supplementary: sensitivity analysis)

We ran sensitivity analyses to assess the effect of changes in the parameter ρ (ρ_0 and ρ_M, the probabilities of being infected by BA.2 and BA.4/5) on our results. To account for uncertainty in a change of parameter ρ during the second surge, we tested increases and decreases of ρ by 5% and 10%.

Changes in parameter ρ significantly influenced the predictive results. Increased transmissibility of the virus increased community protection through natural infection, and such an increase could help to avoid some infections in another epidemic surge. The input into the model of strengthened transmissibility of the virus did not lead to good predictions of the general trend of the second surge (Supplementary Fig. S3AB). The model showed that weakened transmissibility of the virus would delay the peak date and slow the rise in the daily number of cases (Supplementary Figure S3CD).

4. Conclusion and discussion

The study demonstrated that incorporating fine-scale waning immunity into modelling could produce accurate forecasts of the vaccination rates and the second surge of the outbreak. The model developed here simulated daily changes in levels of vaccine protection over time among vaccinated individuals, rather than a single protective status (e.g. a reduced, fixed level of protection). This approach, implemented through discrete-time simulation, overcame the limitation of classical compartmental models in calculating both the dynamics of vaccine-induced immunity and the number of people eligible to receive the next dose.

In addition to immune escape, the comparison of the predictions between the models with waning and constant immunity suggested that vaccine's waning protection was a key factor that shaped this second surge, which involved both BA.2 and BA.4/5. Without the effect of vaccine waning, the surge would have been dominated by delayed but larger spreads of BA.4/5 compared with what happened (Fig. 4F). Other factors, such as temperature and population mobility, had limited influence on the second surge. The winter temperatures were likely to have enhanced virus transmission significantly during the early period of the fifth wave (Supplementary Fig. S1A). Warmer temperatures around September were less likely to be the main driver. Moreover, when the mobility index was reduced in the model, the peak of the fifth epidemic wave was maintained. After mid-April 2022, in reality, the mobility index continued to rise, reaching about 90% of the pre-pandemic level by the end of June (Supplementary Fig. S1B), but the number of daily cases remained low (Fig. 4D). These data indicate that the second surge did not result mainly from the temperature change or the relaxation of social distancing measures.

Although increased vaccine coverage can reduce infection incidence during certain periods (Imai et al., 2023), our data suggest that when immune-escape variants co-circulate, the maintenance of strong vaccine protection may ultimately cause a larger second surge that is dominated by the escape variant. This can be explained by the reduced cross-protection from natural infection with the original strain against the immune-escape variants. Hence, when a strategy of vaccination (or the timing of vaccination) is designed, the pattern of waning immunity should be considered along with other factors, such as immune-escape and disease severity, to achieve long-term benefits (Liu & Lou, 2022).

Even though the model successfully predicted the second surge, we found that the actual number of reported cases reduced more rapidly after the epidemic peak was reached than the numbers predicted in our model. This discrepancy may be due to various factors. First, people may have taken some precautionary measures to protect themselves during the growth of the outbreak. Second, some policies were introduced that would have helped control the epidemic. For example, a "Vaccine Pass" required citizens to receive three doses of the COVID-19 vaccine as soon as possible (The Government of Hong Kong Special Administrative Region, 2022c). Furthermore, the detection rate may have fallen after the end of the initial Omicron outbreak.

Our study contained certain limitations. First, we assumed that individuals who recovered from COVID-19 had strong immunity during the study period, whereas they may have been re-infected a long time later (Kojima & Klausner, 2022; Kwok et al., 2021). Second, the vaccine was assumed to be equally protective across different age groups. However, certain groups of people, such as the elderly, pregnant women and children, can be more susceptible to COVID-19. Third, the model did not account for the fourth dose, which was significant to obtain higher vaccine protection across the population (Bar-On et al., 2022; Gazit et al., 2022). The fourth dose provided little coverage during the study period, reaching about 7.2% of the total population (DATA.GOV.HK., 2022).

Data and material availability

The data that supported this article may be available upon reasonable request to the corresponding author.

CRediT authorship contribution statement

Yuling Zou: Writing – review & editing, Writing – original draft, Validation, Software, Methodology, Formal analysis, Data curation. **Wing-Cheong Lo:** Writing – review & editing, Methodology, Conceptualization. **Wai-Kit Ming:** Writing – review & editing, Supervision. **Hsiang-Yu Yuan:** Writing – review & editing, Validation, Supervision, Project administration, Methodology.

Declaration of competing interest

The authors declare that they have no known competing financial interests or personal relationships that could have appeared to influence the work reported in this paper.

Funding and Acknowledgement

The authors gratefully acknowledge the support from grants funded by the City University of Hong Kong [#7005523, #7005748 and #7005876] and the General Research Fund [#11203823] from the Research Grants Council of Hong Kong. We thank Prof. Joseph T. Wu at the School of Public Health, Li Ka Shing Faculty of Medicine, University of Hong Kong, for his valuable comments, which greatly enhanced the quality of our research.

Appendix A. Supplementary data

Supplementary data to this article can be found online at https://doi.org/10.1016/j.idm.2024.09.006.

References

Bar-On, Y. M., Goldberg, Y., Mandel, M., Bodenheimer, O., Amir, O., Freedman, L., Alroy-Preis, S., Ash, N., Huppert, A., & Milo, R. (2022). Protection by a fourth dose of BNT162b2 against Omicron in Israel. *New England Journal of Medicine, 386*(18), 1712–1720. https://doi.org/10.1056/NEJMoa2201570

Bubar, K. M., Reinholt, K., Kissler, S. M., Lipsitch, M., Cobey, S., Grad, Y. H., & Larremore, D. B. (2021). Model-informed COVID-19 vaccine prioritization strategies by age and serostatus. *Science (New York, N.Y.), 371*(6532), 916–921. https://doi.org/10.1126/science.abe6959

Chen, X., Bai, X., Chen, X., Zheng, N., Yang, J., Zhang, J., & Yu, H. (2023). Modeling the prediction on the efficacy of a homologous third dose of CoronaVac against SARS-CoV-2 Omicron BA.1, BA.2, BA.2.12.1, and BA.4/5 - China, 2020-2021. *China CDC Weekly, 5*(5), 103–107. https://doi.org/10.46234/ccdcw2023.019

DATA.GOV.HK.. (2022). Daily count of vaccination by age groups. Available from: https://data.gov.hk/en-data/dataset/hk-hhb-hhbcovid19-vaccination-rates-over-time-by-age. (Accessed 31 October 2022).

Department of Health. (2022). The government of Hong Kong special administrative region. Available from: https://www.dh.gov.hk/english/index.html. (Accessed 31 October 2022).

Dick, D. W., Childs, L., Feng, Z., Li, J., Röst, G., Buckeridge, D. L., Ogden, N. H., & Heffernan, J. M. (2021). COVID-19 seroprevalence in Canada modelling waning and boosting COVID-19 immunity in Canada a Canadian immunization Research network study. *Vaccines, 10*(1), 17. https://doi.org/10.3390/vaccines10010017

Esterman, A. (2022). New Covid subvariants BA.4 and BA.5 are the most contagious yet – and driving Australia's third Omicron wave. Available from: https://www.theguardian.com/world/2022/jul/05/new-covid-variants-ba4-ba5-most-contagious-australia-third-omicron-wave-coronavirus-sub-variants-ba-4-5. (Accessed 5 July 2022).

Gazit, S., Saciuk, Y., Perez, G., Peretz, A., Pitzer, V. E., & Patalon, T. (2022). Short term, relative effectiveness of four doses versus three doses of BNT162b2 vaccine in people aged 60 years and older in Israel: Retrospective, test negative, case-control study. *BMJ, 377*, Article e071113. https://doi.org/10.1136/bmj-2022-071113

He, S., Peng, Y., & Sun, K. (2020). SEIR modeling of the COVID-19 and its dynamics. *Nonlinear Dynamics, 101*(3), 1667–1680. https://doi.org/10.1007/s11071-020-05743-y

Imai, N., Rawson, T., Knock, E. S., Sonabend, R., Elmaci, Y., Perez-Guzman, P. N., Whittles, L. K., Kanapram, D. T., Gaythorpe, K. A. M., Hinsley, W., Djaafara, B. A., Wang, H., Fraser, K., FitzJohn, R. G., Hogan, A. B., Doohan, P., Ghani, A. C., Ferguson, N. M., Baguelin, M., & Cori, A. (2023). Quantifying the effect of delaying the second COVID-19 vaccine dose in england: A mathematical modelling study. *The Lancet Public Health, 8*(3), e174–e183. https://doi.org/10.1016/S2468-2667(22)00337-1

Khoury, D. S., Cromer, D., Reynaldi, A., Schlub, T. E., Wheatley, A. K., Juno, J. A., Subbarao, K., Kent, S. J., Triccas, J. A., & Davenport, M. P. (2021). Neutralizing antibody levels are highly predictive of immune protection from symptomatic SARS-CoV-2 infection. *Nature Medicine, 27*(7), 1205–1211. https://doi.org/10.1038/s41591-021-01377-8

Kojima, N., & Klausner, J. D. (2022). Protective immunity after recovery from SARS-CoV-2 infection. *The Lancet Infectious Diseases, 22*(1), 12–14. https://doi.org/10.1016/S1473-3099(21)00676-9

Kwok, K. O., Li, K. K., Tang, A., Tsoi, M. T. F., Chan, E. Y. Y., Tang, J. W. T., Wong, A., Wei, W. I., & Wong, S. Y. S. (2021). Psychobehavioral responses and likelihood of receiving COVID-19 vaccines during the pandemic, Hong Kong. *Emerging Infectious Diseases, 27*(7), 1802–1810. https://doi.org/10.3201/eid2707.210054

Lau, J. J., Cheng, S. M. S., Leung, K., Lee, C. K., Hachim, A., Tsang, L. C. H., Yam, K. W. H., Chaothai, S., Kwan, K. K. H., Chai, Z. Y. H., Lo, T. H. K., Mori, M., Wu, C., Valkenburg, S. A., Amarasinghe, G. K., Lau, E. H. Y., Hui, D. S. C., Leung, G. M., Peiris, M., & Wu, J. T. (2024). Author Correction: Real-world COVID-19 vaccine effectiveness against the Omicron BA.2 variant in a SARS-CoV-2 infection-naive population. *Nature Medicine, 30*(1), 305. https://doi.org/10.1038/s41591-023-02648-2

Levin, E. G., Lustig, Y., Cohen, C., Fluss, R., Indenbaum, V., Amit, S., Doolman, R., Asraf, K., Mendelson, E., Ziv, A., Rubin, C., Freedman, L., Kreiss, Y., & Regev-Yochay, G. (2021). Waning immune humoral response to BNT162b2 covid-19 vaccine over 6 months. *New England Journal of Medicine, 385*(24), e84. https://doi.org/10.1056/NEJMoa2114583

Liang, J. B., Yuan, H. Y., Li, K. K., Wei, W. I., Wong, S. Y. S., Tang, A., Riley, S., & Kwok, K. O. (2022). Path to normality: Assessing the level of social-distancing measures relaxation against antibody-resistant SARS-CoV-2 variants in a partially-vaccinated population. *Computational and Structural Biotechnology Journal, 20*, 4052–4059. https://doi.org/10.1016/j.csbj.2022.07.048

Liu, K., & Lou, Y. (2022). Optimizing COVID-19 vaccination programs during vaccine shortages. *Infectious Disease Modelling, 7*(1), 286–298. https://doi.org/10.1016/j.idm.2022.02.002

Liu, Y., Pearson, C. A. B., Sandmann, F. G., Barnard, R. C., Kim, J. H., Flasche, S., Jit, M., Abbas, K., & Cmmid Covid-19 Working Group. (2022). Dosing interval strategies for two-dose COVID-19 vaccination in 13 middle-income countries of Europe: Health impact modelling and benefit-risk analysis. *The Lancet Regional Health. Europe, 17*, Article 100381. https://doi.org/10.1016/j.lanepe.2022.100381

Mahmud, M. S., Kamrujjaman, M., Adan, M. M. Y., Hossain, M. A., Rahman, M. M., Islam, M. S., Mohebujjaman, M., & Molla, M. M. (2022). Vaccine efficacy and SARS-CoV-2 control in California and U.S. During the session 2020-2026: A modeling study. *Infectious Disease Modelling, 7*(1), 62–81. https://doi.org/10.1016/j.idm.2021.11.002

Menegale, F., Manica, M., Zardini, A., Guzzetta, G., Marziano, V., d'Andrea, V., Trentini, F., Ajelli, M., Poletti, P., & Merler, S. (2023). Evaluation of waning of SARS-CoV-2 vaccine-induced immunity: A systematic review and meta-analysis. *JAMA Network Open, 6*(5), Article e2310650. https://doi.org/10.1001/jamanetworkopen.2023.10650

Najar, F. Z., Linde, E., Murphy, C. L., Borin, V. A., Wang, H., Haider, S., & Agarwal, P. K. (2023). Future COVID19 surges prediction based on SARS-CoV-2 mutations surveillance. *Elife, 12*, Article e82980. https://doi.org/10.7554/eLife.82980

Our World in Data. (2022). How did the number of visitors change since the beginning of the pandemic? Hong Kong. Available from: https://ourworldindata.org/grapher/changes-visitors-covid?country=~HKG. (Accessed 15 October 2022).

Peng, Q., Zhou, R., Wang, Y., Zhao, M., Liu, N., Li, S., Huang, H., Yang, D., Au, K. K., Wang, H., Man, K., Yuen, K. Y., & Chen, Z. (2022). Waning immune responses against SARS-CoV-2 variants of concern among vaccinees in Hong Kong. *EBioMedicine, 77*, Article 103904. https://doi.org/10.1016/j.ebiom.2022.103904

Pérez-Then, E., Lucas, C., Monteiro, V. S., Miric, M., Brache, V., Cochon, L., Vogels, C. B. F., Malik, A. A., De la Cruz, E., Jorge, A., De Los Santos, M., Leon, P., Breban, M. I., Billig, K., Yildirim, I., Pearson, C., Downing, R., Gagnon, E., Muyombwe, A., Razeq, J., … Iwasaki, A. (2022). Neutralizing antibodies against the SARS-CoV-2 Delta and Omicron variants following heterologous CoronaVac plus BNT162b2 booster vaccination. *Nature Medicine, 28*(3), 481–485. https://doi.org/10.1038/s41591-022-01705-6

Smith, T. P., Flaxman, S., Gallinat, A. S., Kinosian, S. P., Stemkovski, M., Unwin, H. J. T., Watson, O. J., Whittaker, C., Cattarino, L., Dorigatti, I., Tristem, M., & Pearse, W. D. (2021). Temperature and population density influence SARS-CoV-2 transmission in the absence of nonpharmaceutical interventions. *Proceedings of the National Academy of Sciences of the United States of America, 118*(25), Article e284118. https://doi.org/10.1073/pnas.2019284118

The Government of Hong Kong Special Administrative Region. (2022a). CHP investigates locally acquired SARS-CoV-2 virus cases with 1 052 cases tested positive by nucleic acid tests and 2 929 cases by RATs as well as 437 imported cases. Available from: https://www.info.gov.hk/gia/general/202211/01/P2022110100517.htm. (Accessed 1 December 2022).

The Government of Hong Kong Special Administrative Region. (2022b). COVID-19 thematic website - together, we fight the virus. Available from: https://www.coronavirus.gov.hk/eng/index.html. (Accessed 31 October 2022).

The Government of Hong Kong Special Administrative Region. (2022c). Vaccine pass. Available from: https://www.coronavirus.gov.hk/eng/vaccine-pass.html. (Accessed 29 December 2022).

The Government of Hong Kong Special Administrative Region. (2022). Announcement of appointment arrangements for shortened intervals between COVID-19 vaccine doses. Available from: https://www.info.gov.hk/gia/general/202203/04/P2022030400691.htm. (Accessed 4 March 2022).

Thompson, M. G., Burgess, J. L., Naleway, A. L., Tyner, H. L., Yoon, S. K., Meece, J., Olsho, L. E. W., Caban-Martinez, A. J., Fowlkes, A., Lutrick, K., Kuntz, J. L., Dunnigan, K., Odean, M. J., Hegmann, K. T., Stefanski, E., Edwards, L. J., Schaefer-Solle, N., Grant, L., Ellingson, K., Groom, H. C., … Gaglani, M. (2021). Interim estimates of vaccine effectiveness of BNT162b2 and mRNA-1273 COVID-19 vaccines in preventing SARS-CoV-2 infection among health care personnel, first responders, and other essential and frontline workers - eight U.S. Locations, December 2020-March 2021. *Morbidity & Mortality Weekly Report, 70*(13), 495–500. https://doi.org/10.15585/mmwr.mm7013e3

World Health Organization. (2023). Statement on the fifteenth meeting of the IHR (2005) Emergency Committee on the COVID-19 pandemic. Available from: https://www.who.int/news/item/05-05-2023-statement-on-the-fifteenth-meeting-of-the-international-health-regulations-(2005)-emergency-committee-regarding-the-coronavirus-disease-(covid-19)-pandemic. (Accessed 5 May 2023).

Yuan, H. Y., Liang, J., & Hossain, M. P. (2022). Impacts of social distancing, rapid antigen test and vaccination on the Omicron outbreak during large temperature variations in Hong Kong: A modelling study. *Journal of Infection and Public Health, 15*(12), 1427–1435. https://doi.org/10.1016/j.jiph.2022.10.026

Hong Kong Observatory. (2022). Highlight of Hong Kong climate. Available from: https://www.hko.gov.hk/en/cis/climat.htm. (Accessed 31 October 2022).